A Dual-Phase-Shift Control Strategy for Dual-Active-Bridge DC-DC Converter in Wide Voltage Range

Myoungho Kim[1], Martin Rosekeit[2], Seung-Ki Sul[1] and Rik W. A. A. De Doncker[2]

[1] School of Electrical Engineering & Computer Science, Seoul National University
San 56-1, Shillim-Dong, Kwanak-Gu, Seoul, South Korea
[2] Institute for Power Electronics and Electrical Drives, RWTH Aachen University
Jaegerstrasse 17-19, 52066 Aachen, Germany

Abstract--This paper analyzes the dual-phase-shift (DPS) control strategy for a dual-active-bridge (DAB) converter in whole operation range. The DPS has two degree of freedom to control the transferring power, which can improve the performance of the DAB converter than single-phase-shift (SPS) control strategy. This paper derives the reactive power, the rms and the peak current flowing on the transformer and the zero-voltage-switching (ZVS) condition according to the operating conditions. Using this analysis and simulation results, a suitable control strategy for DAB converter is obtained. Experiments are performed to verify the proposed control strategy and to compare with the conventional SPS control strategy. The experimental results show that the proposed method can enhance the overall efficiency and expand the ZVS operation range.

Index Terms--DC-DC converter, double-phase-shift (DPS), dual-active-bridge (DAB), zero-voltage-switching (ZVS).

I. INTRODUCTION

The needs for the isolated bidirectional DC-DC converters are in growing trend. The DC-DC converters are used in various applications, ranging from uninterrupted power supplies (UPS), power converters for the energy storage management system, to electric vehicles. Some DC-DC converter topologies have been investigated for this necessity [1]-[4]. The dual-active-bridge (DAB) converter is one of them. Since proposed in [4], it has been widely used especially for high power applications because of its attractive features such as high power density, simple implementation, low number of passive components and zero-voltage-switching (ZVS) characteristic.

Fig. 1 shows the DAB converter circuit, which consists of two full-bridge on primary and secondary side and a high frequency transformer. The H-bridges synthesize each output voltages applied to the high frequency transformer. The transformer provides galvanic isolation between primary and secondary sides, and matches the voltage difference between two sides. The leakage inductance of the transformer is utilized as an instantaneous energy storage element.

The traditional control method for this topology is single-phase-shift (SPS) control. The output voltages of primary and secondary side (V_p and V_s) form square wave
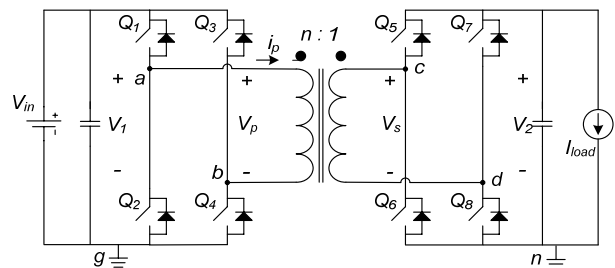

Fig. 1. Dual-Active-Bridge circuit.

with 50% duty ratio and have shifted-phase between two sides. The average transferring power is controlled by adjusting the phase-shift angle. This control strategy is very intuitive and easy to implement. However, this method can only manage the average output power, because it has only one degree of freedom. Other variables are not considered in deciding the phase-shift angle, such as circulating reactive power, current flowing on the transformer, which can deteriorate the system performance.

Accordingly, other control algorithms were developed to improve the system performance [5]-[8]. Basically, they adjust the duty ratio of the output voltages of H-bridges as well as the phase-shift between the primary and secondary side. Triangular modulation (TRM) and Trapezoidal modulation (TZM) are investigated in [5] and [6]. They focused on minimizing the current at turn-off instant of switching devices to reduce the switching loss. However, these methods might rather increase the rms current on the transformer which could increase the overall system loss. Also, they can be implemented only in a condition of limited input-output voltage ratio and low power range. Ref. [7] proposed composition method of TRM/TZM and SPS control. It switches modulation method according to the operation condition, so it provided a way to apply TRM/TZM to applications which have wide operation range. But still, the other variables, such as rms current, are not considered. In [8], dual-phase-shift (DPS) algorithm is analyzed. It provides more general way to synthesizing the output voltages, by adjusting the duty ratios of output voltages of H-bridges. However, its analysis is mainly focused on minimizing the reactive power and the efficiency is not fully

considered. Also, the algorithm for reducing the reactive power has fairy limited operation range.

This paper makes an analysis of DPS algorithm for DAB converter in whole operation range. It covers wide voltage ratio of primary and secondary side DC-link, and whole possible duty ratio and phase-shift angle. The average output power, the reactive power, and the rms and the peak current flowing on the transformer are analytically investigated. ZVS condition according to the switching state is also examined. The analysis is verified with simulations and experiments.
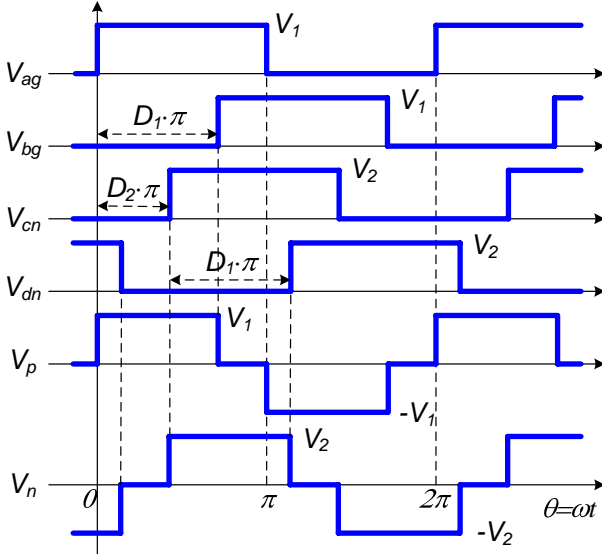
II. ANALYSIS OF DPS CONTROL

Fig. 2. Voltage waveforms of DPS control.

Fig. 2 shows the DPS control strategy. It controls two phase-shift angles, phase-shift between half-bridges in the identical side and between primary and secondary side. Extents of each phase-shift are defined as D_1 and D_2, and their ranges are from zero to one. As the result, duty ratios of primary and secondary output voltage, V_p and V_n, can be adjusted as well as the phase-shift angle between them. The conventional SPS control can be regarded as a specific part of DPS control which set D_1 to one. With this definition, the output power can be deduced.
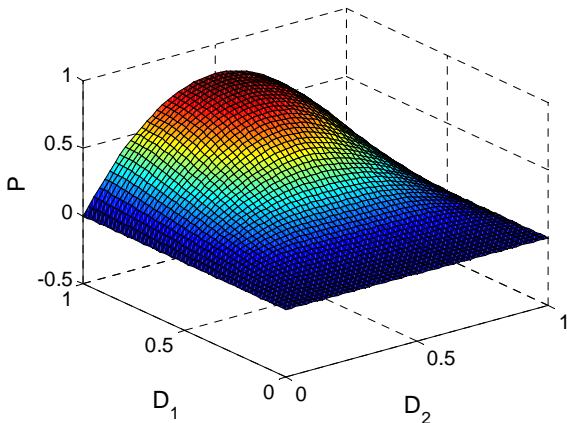

Fig. 3. Average output power according to the phase-shift pair.

Fig. 3 shows the average output power plane of DPS control according to phase-shift pair (D_1 and D_2). All quantities in this section are normalized by following base values.

$$V_b = V_1, \quad I_b = \frac{V_1}{\omega L}, \quad P_b = V_b I_b = \frac{V_1^2}{\omega L}. \tag{1}$$

Eq. (2) presents the average output power formula. The average output power is varied according to D_1 and D_2. Other variables, d, V_1, f_s, and L_s only affect overall magnitude. And except D_1 and D_2, other variables are given operating condition, which cannot be manipulated. Therefore, a proper selection of phase-shift pair is required in order to yield certain amount of output power. In Fig. 3, the maximum output power is produced at the case of D_1=1 and D_2=0.5, which is the same as the case of SPS control. However, for other value of output power, infinite combinations of D_1 and D_2 can be selected. Therefore a criterion is required to select a combination of phase-shift pair for a certain output power. For that, this paper analyzes some performance indices; reactive power, rms and peak current flowing on the transformer and zero-voltage-switching (ZVS) condition are them.

The reactive power stands for the power transferred in reverse direction to the average output power, defined in [8]. Because the DAB converter uses leakage inductance of the transformer, phases of voltage and current are not always coincide. Therefore the sign of voltage and current can be different in some period, and the power occurred in this period has different sign from that of average power. The power of this part is defined as the reactive power. The reactive power makes instantaneous fluctuation on output power of the DAB converter, and this causes the voltage and current fluctuation at the DC-link. The fluctuation should be absorbed by the DC-link capacitor. In order to reduce the voltage fluctuation, larger DC-link capacitor is required, and the current ripple induces loss by equivalent series resistance of the capacitor. Hence, less reactive power is desirable. In DPS control, the magnitude of reactive power can be derived as (3). Unlike the case of the average output power, voltage ratio between the primary side and the secondary side (d) affects the shape of the reactive power with phase-shift pair. Fig.4 shows the reactive power plane according to the phase-shift pair in some conditions of the voltage ratio.

In order to reduce loss, the current should be considered also. Generally, the loss in the converter occurs in the transformer and switching devices. Again, the loss of the transformer is divided into the core loss and copper loss, and the loss of the switching device consists of the switching loss and the conduction loss. The copper loss of the transformer and the conduction loss of the switching device are, both, proportional to the rms current on the transformer. Thus, less rms current for the same output power is advantageous to reduce the copper loss. Eq. (4) presents the magnitude of rms current in DPS control, and Fig. 5 shows the rms current plane according to the phase-shift pair in some conditions of the voltage ratio.

$$P = \frac{dV_1^2}{4f_sL_s} \times \begin{cases} D_2(2D_1 - D_2), & when \ D_2 < D_1 \ and \ D_1 + D_2 \le 1 \\ (2D_2 + 2D_1 - 1 - 2D_2^2 - D_1^2), & when \ D_2 < D_1 \ and \ D_1 + D_2 > 1 \\ D_1^2, & when \ D_2 \ge D_1 \ and \ D_1 + D_2 \le 1 \\ (2D_1 - D_2^2 + 2D_2 - 2D_2D_1 - 1), & when \ D_2 \ge D_1 \ and \ D_1 + D_2 > 1 \end{cases} . \tag{2}$$

$$Q = \frac{V_1^2}{16f_sL_s} \times \begin{cases} \dfrac{D_1(d+1)\{D_1(d+1) + 4d(D_2-1)\} + 4d^2(D_2-1)^2}{d+1}, \\ \quad when \ d \ge 1 \ \& \ 2d(D_2-1)+(1+d)D_1 \ge 0 \ or \ d < 1 \ \& \ 2(D_2-1)+(1+d)D_1 \ge 0 \\ 0, \quad when \ d \ge 1 \ \& \ 2d(D_2-1)+(1+d)D_1 < 0 \ \& \ 2dD_2+(1-d)D1 \ge 0 \\ \dfrac{4dD_2\{dD_2 - D_1(d-1) + 4d(D_2-1)\} + 4d^2(D_2-1)^2}{d-1}, \quad when \ d \ge 1 \ \& \ 2dD_2+(1-d)D1 < 0 \\ \{D_1^2(d+1)^2 + 4d(D_2-1)(2D_1+D_2-1)\}, \\ \quad when \ 2(D_2-1)+(1+d)D_1 < 0 \ \& \ D_1+D_2 \ge 1 \ \& \ 2D_2+(d-1)D_1 \ge 0 \\ D_1^2(d-1)^2, \quad when \ 2D_2+(d-1)D_1 \ge 0 \ \& \ d < 1 \ \& \ D_1+D_2 \ge 1 \\ \dfrac{D_1^2(3d+1)(d-1) + 4d(d-1)(D_1D_2 - 2D_1 + 1) + 4dD_2\{D_2(d-2)-2d+2\}}{d-1}, \\ \quad when \ D_1+D_2 \ge 1 \ \& \ 2D_2+(d-1)D_1 < 0 \\ \dfrac{4dD_2\{D_2 + D_1(d-1)\} + D_1^2(d-1)^2}{1-d}, \quad when \ d < 1 \ \& \ D_1+D_2 < 1 \ \& \ 2D_2+(d-1)D_1 < 0 \end{cases} . \tag{3}$$

$$I_{RMS} = \frac{\sqrt{3}V_1}{12f_sL_s} \times \begin{cases} \sqrt{D_1^2(d-1)^2(3-2D_1) - 4dD_2^2(D_2-3D_1)}, & when \ D_2 < D_1 \ \& \ D_1+D_2 \le 1, \\ \sqrt{-2D_1^3(d^2+1) + 3D_1^2(d+1)^2 - 12dD_2(D_1-1)^2 - 4dD_2^2(2D_2-3) - 4d(3D_1-1)}, \\ & when \ D_2 < D_1 \ \& \ D_1+D_2 > 1 \\ D_1\sqrt{3(d-1)^2 - 2D_1(d+1) + 12dD_2}, & when \ D_2 \ge D_1 \ \& \ D_1+D_2 \le 1 \\ \sqrt{D_1^2(3-2D_1)(d+1)^2 - 4d(D_2-1)^2(D_2+3D_1-1)}, & when \ D_2 \ge D_1 \ \& \ D_1+D_2 > 1 \end{cases} . \tag{4}$$

$$I_{peak} = \frac{V_1^2}{4f_sL_s} \times \begin{cases} D_2 + dD_1 + |1-d|(D_1 - D_2), & when \ D_2 \le D_1 \\ D_1(1+d), & when \ D_2 > D_1 \end{cases} . \tag{5}$$

where f_s is the switching frequency, V_1 is primary side DC-link voltage, d is voltage ratio between the primary and secondary side, ($d = nV_2/V_1$, n is turn ratio of the transformer), L_s is the leakage inductance of the transformer.
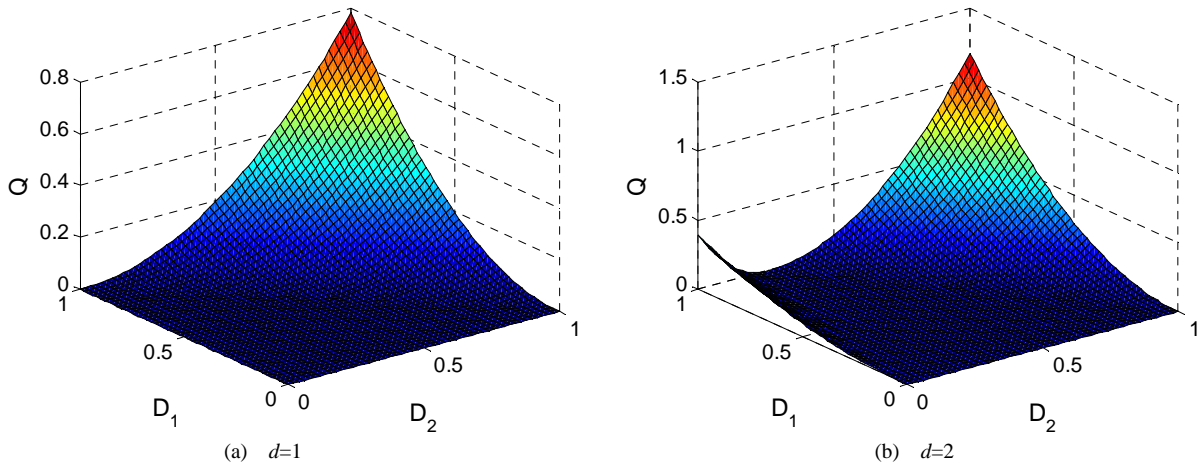

(a) $d=1$ (b) $d=2$
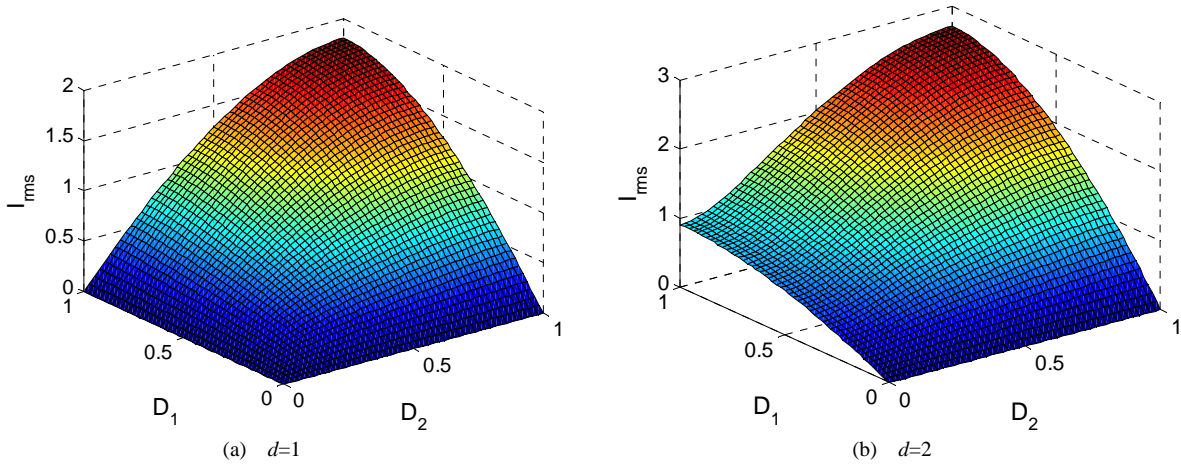
Fig. 4. Reactive power according to the phase-shift pair.

(a) $d=1$ (b) $d=2$

Fig. 5. Rms current according to the phase-shift pair.
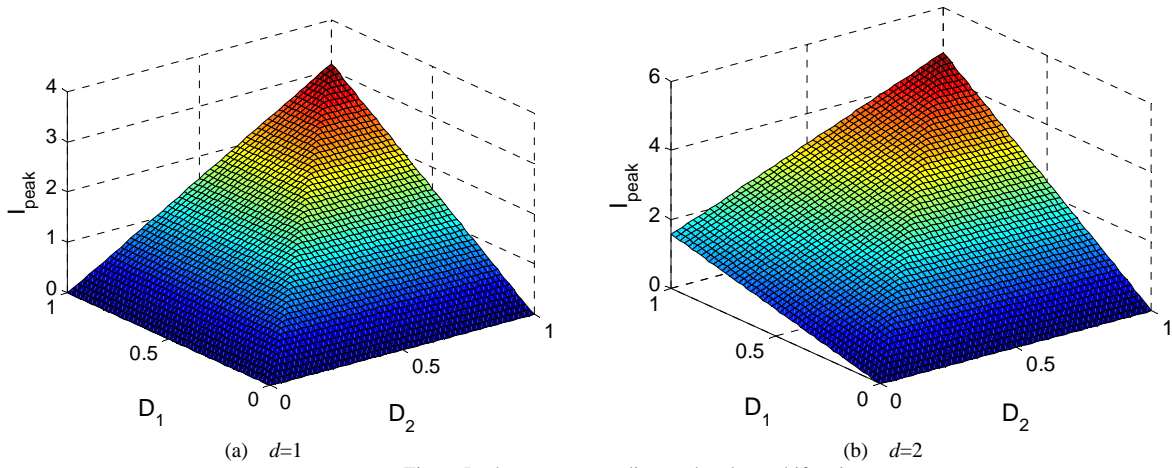

(a) $d=1$ (b) $d=2$

Fig. 6. Peak current according to the phase-shift pair.

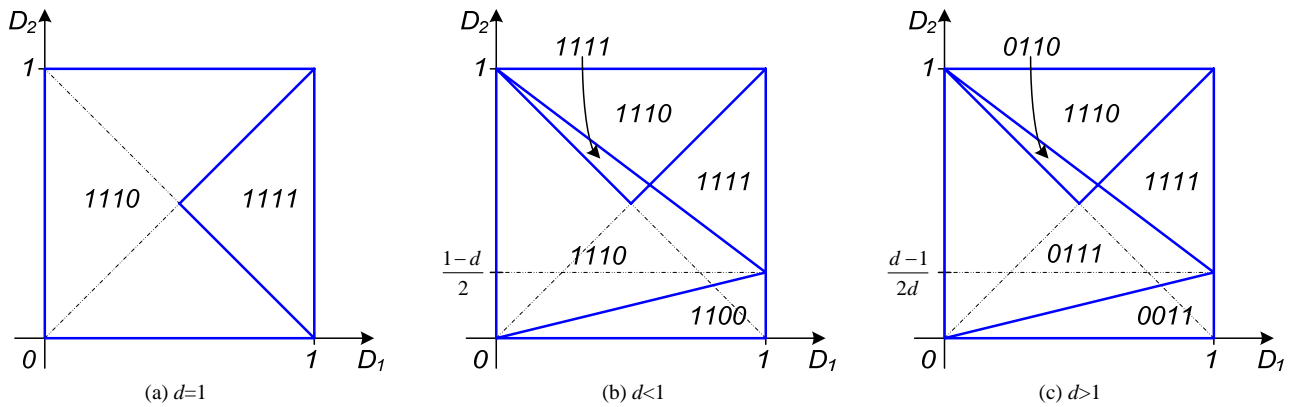(a) $d=1$ (b) $d<1$ (c) $d>1$

Fig. 7. ZVS condition according to the phase-shift pair

The core loss of the transformer consists of hysteresis and eddy-current loss, and both can be presented as functions of the maximum flux density applied to the core. The maximum flux density is almost proportional to the net voltage-second applied to the transformer, which is also proportional to the magnitude of peak current on the transformer. Therefore the larger peak current results in larger core loss. The magnitude of peak current is also related to the switching loss. The turn off loss of the switching device is determined by the current magnitude at the switching instants, and the current reaches its peak value at the switching instants. Accordingly, the magnitude of peak current is related to the converter loss. The magnitude of peak current is derived in (5) and the plane of peak current is shown in Fig. 6.

The ZVS is one of merits of DAB converter. However, it is not always achieved. In SPS strategy, the condition for the ZVS depends on the voltage ratio, and the phase-shift angle [9]. Like the case of SPS, the ZVS is also not always achieved in DPS control strategy. The ZVS

condition is determined by the current directions at the switching moments, which are functions of d, D_1 and D_2. This paper analyzes the ZVS condition of each switch (Q_1 to Q_8 on Fig. 1). Fig. 7 shows the ZVS condition in 4-bit representation according to the phase-shift pair. Each bit stands for availability of ZVS for one leg. The most left bit is corresponded to Q_1 and Q_2, and the left second bit is for Q_3 and Q_4. Each bit is matched in this way. For each bit, '1' means that ZVS is achieved and '0' means ZVS is not achieved.

When the voltage ratio is unity, ZVS is achieved on all legs in SPS control (D_1 is set to 1) for entire power range. But as the voltage ratio varies, the operation range where all four legs turn on zero-voltage decreases. In low power range (small D_2), ZVS is done on only two legs. In this case, DPS control can help increasing number of legs which perform ZVS. Under the assumption that the voltage ratio is two and the output power is low enough, then the ZVS condition is '0011'. In this case, by properly selecting the phase-shift pair, (reducing D_1 and increasing D_2), ZVS condition can be moved to '0111' maintaining the same output power. Then one more leg would be operated in soft-switching condition.

III. CONTROL STRATEGY

Using the performance indices derived in former section, the phase-shift pair can be selected. As described in (3) – (5), they are varied by the phase-shift pair and voltage ratio, while the other variables are only concerned with the overall magnitude of them. Also, the voltage ratio is not a controllable variable, but a given condition. Hence, only the phase-shift pair is able to be adjusted. First of all, the output power plane is symmetric about the line $D_2=0.5$ as shown in Fig. 3. And all the other performance indices, the reactive power, the rms and the peak current have significantly lower values in the area of $D_2 \leq 0.5$. Hence, it is adequate to limit the maximum range of D_2 up to 0.5. Then, given the output power reference and the target performance index, a proper phase-shift pair is selected, which satisfies producing the reference output power and minimizing the corresponding

performance index.

The trajectory of phase-shift pair can be obtained by using (2) - (5). Each performance index has its minimum value at the point where the output power plane and the performance index plane meet. Therefore, the optimum phase-shift pair tracks the points where the gradients of the output power and the performance index are parallel in D_1 and D_2 coordination. And, the phase-shift pair for the minimum peak current can be derived as (6).

The phase-shift trajectory for the minimum peak current can be deduced in this way, but this method is difficult to apply to the trajectory for the minimum rms current and reactive power. Since their formulas are too complex to calculate analytically. Instead of analytic solution, this paper makes the look-up tables combining (2) - (4) and employs them to find the phase-shift pairs for the minimum rms current and reactive power.

Fig. 8 shows the optimum trajectory of the phase-shift pair for each performance index with some voltage ratio
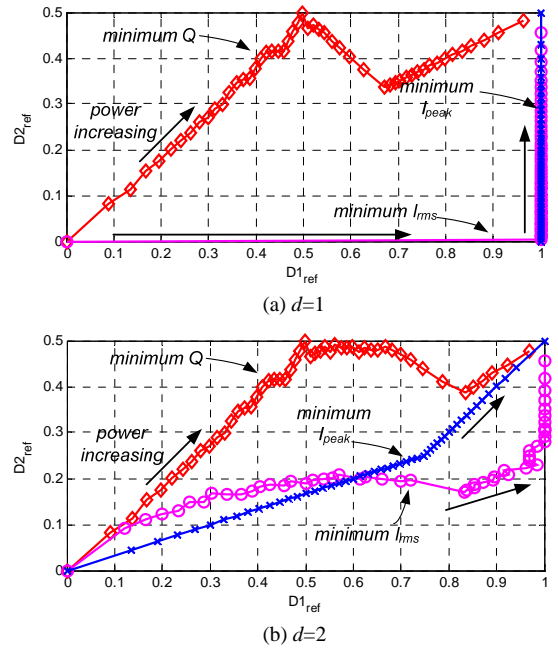

(a) $d=1$

(b) $d=2$

Fig. 8. Trajectory of phase-shift pairs for minimum performance indices

$$\left(D_1, D_2\right) \text{ which satisfies } \left(\frac{\partial I_{peak}}{\partial D_1}, \frac{\partial I_{peak}}{\partial D_2}\right) = \left(\frac{\partial P}{\partial D_1}, \frac{\partial P}{\partial D_2}\right),$$

$$D_2 = \frac{2}{V_1}\sqrt{\frac{PL_s f_s(1-d)}{d(1+3d)}}, \ D_1 = \frac{D_2(1+d)}{1-d}, \qquad\qquad \text{when } d<1, D_2 < D_1 \text{ and } D_1 + D_2 \leq 1$$

$$D_2 = \frac{2}{V_1}\sqrt{\frac{PL_s f_s(d-1)}{d(3+d)}}, \ D_1 = \frac{D_2(1+d)}{d-1}, \qquad\qquad \text{when } d \geq 1, D_2 < D_1 \text{ and } D_1 + D_2 \leq 1$$

$$D_2 = \frac{A_1 - \sqrt{A_1^2 - 4A_1\left\{(1-d)^2 + B_1\right\}}}{2A_1}, D_1 = \frac{2D_2 - 2dD_2 - 1 + 3d}{2d}, \text{ when } d<1, D_2 < D_1 \text{ and } D_1 + D_2 > 1$$

(6)

$$D_2 = \frac{A_2 - \sqrt{A_2^2 - 4A_2\left\{(1-d)^2 + B_2\right\}}}{2A_2}, D_1 = \frac{3dD_2}{2} - D_2 - \frac{1}{2}d, \qquad \text{when } d \geq 1, D_2 < D_1 \text{ and } D_1 + D_2 > 1$$

$$\text{where } A_1 = 4(3d^2 - 2d + 1), \ A_2 = 4(d^2 - 2d + 3), \ B_1 = \frac{16df_s L_s P}{V_1^2}, \ B_2 = \frac{16f_s L_s P}{V_1^2}.$$

values. If the voltage ratio is unity, phase-shift trajectories for the minimum rms and peak current is the same with the SPS control strategy (D_1 is set to 1). In other cases, trajectories for optimizing each performance index are quite different. Therefore it is not possible to maintain all performance indices as minimum concurrently, and one of them should be chosen as a main target.

IV. SIMULATION RESULTS

This paper performs simulations to verify the DPS control strategy and compare the performance depending on the phase-shift pair trajectories. A battery charging/discharging system for electric vehicles is employed as a model for the simulation. The simulation model is developed in the simulation tool Matlab/Simulink and Plecs. The parameters of DAB used in the simulation model are shown in Table 1.

TABLE I
PARAMETERS OF THE DAB CONVERTER

Rated power	3.68 kW
DC-link voltage	200 V – 350 V at primary side
	350 V - 400 V at secondary side
Switching frequency	50 kHz
Transformer turn ratio	16 : 18
Leakage inductance of the transformer	43 μH

The simulation is performed under a condition of the largest voltage ratio in the system specification (d=1.78, $V_1 = 200V$, $V_2 = 400V$) maximize the difference of the effect of control strategy. The reactive power, the rms current, and the overall efficiency are calculated using SPS control strategy and three DPS trajectories while from 10% to 100% of the rated power is applied.

The loss model of the system consists of the conduction loss of the transformer and the switching and conduction loss of the switching devices. The loss model of switching device is made by referring to its datasheet (F4-75R06W1E3, IGBT module of Infineon). The core loss of the transformer is neglected.

Fig. 9 shows the simulation results. As the analysis in former section, the reactive power is minimum with DPS-Q, and the rms current is minimum with DPS-I_{rms}. Both show much better results than the case of SPS. And the results with DPS-I_{peak} approximately lie between two other DPS trajectories. This can be explained with the trajectories, shown on Fig. 8. DPS-I_{peak} is placed between the other DPS trajectories when the output power is more than around 50% of the rated value. And the differences of the rms current and the reactive power between the DPS-I_{rms} and the DPS-I_{peak} are not significant in the lower power region. Therefore, the control strategy could be chosen according which performance index is regarded as important one in target applications.
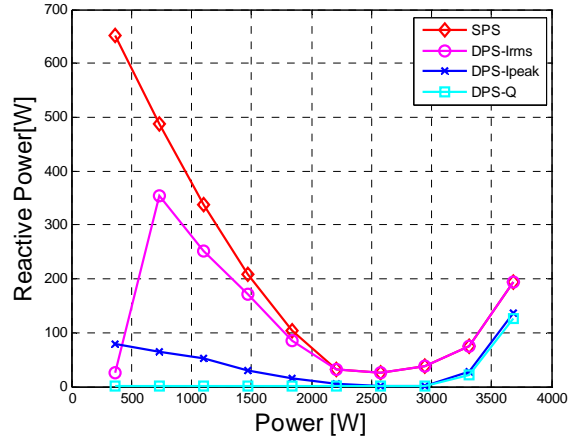
However, the DPS-Q is not suitable for general applications, because of its low efficiency. The system efficiency depends on the rms and the peak current, which affects the conduction and switching loss, respectively. The case of DPS-Q shows the worst result,
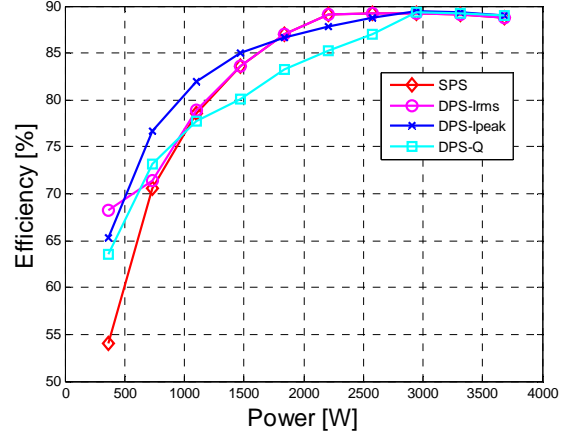
(a) reactive power
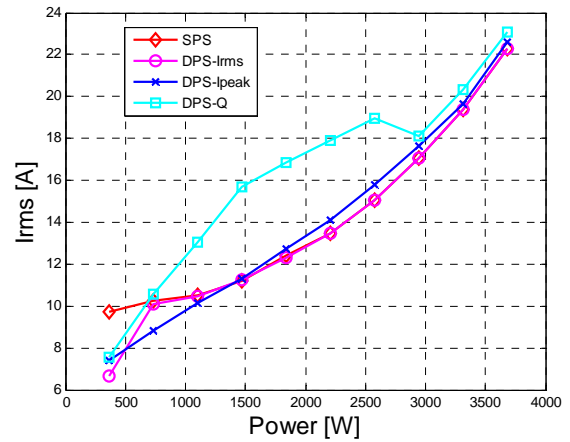
(b) rms current

(c) efficiency
Fig. 9. Efficiency comparison of SPS and DPS-I_{peak}

even than the case of SPS in high power range because the rms current in case of DPS-Q is larger.

The results of DPS-I_{rms} and DPS-I_{peak} are comparable. As the rms current is slightly less in the case of DPS-I_{rms}, the conduction loss of it is less than the case of DPS-I_{peak}. However, because the less peak current of the case of DPS-I_{peak}, it would reveal less switching loss. The overall efficiency would be determined by the proportion between the conduction and the switching loss of the
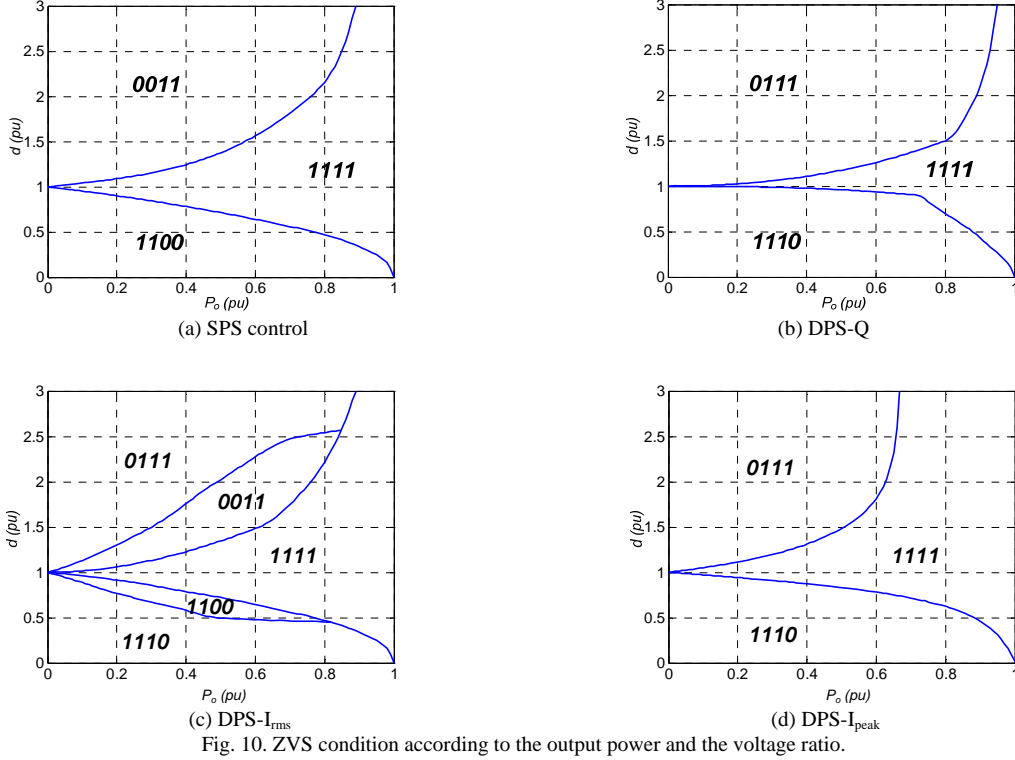
Fig. 10. ZVS condition according to the output power and the voltage ratio.

system. However, the DPS-I$_{peak}$ shows better result than DPS-I$_{rms}$ does in the aspect of the reactive power.

Also, DPS-I$_{peak}$ is advantageous in terms of ZVS condition. Fig. 10 shows the ZVS condition in 4-bit representation according to the output power and the voltage ratio with each control strategy. The output power in the figure is normalized by the maximum output power. Generally, DPS control strategies result in wider ZVS operating range. When the voltage ratio is not unity, three legs of the DAB converter perform ZVS with DPS control, while the only two legs perform ZVS with SPS control. Among the DPS strategies, DPS-I$_{peak}$ presents most desirable result. DPS-Q has relatively small area of '1111', where all legs of the converter is achieved ZVS. And DPS-I$_{peak}$ has '1100' and '0011' area where only two legs can achieve ZVS. As the voltage ratio is around unity, DPS-I$_{rms}$ passes through these parts. Therefore, smaller number of switches performs soft-switching in some power range with DPS-I$_{rms}$ or DPS-Q comparing to the case of DPS-I$_{peak}$.

Consequently, the DPS-I$_{peak}$ would be adequate for general solution. It results in reasonable efficiency and reduced reactive power, and wider ZVS range. Also, it is relatively easy to implement among the DPS control strategies.

V. EXPERIMENTAL RESULTS

A prototype of battery charging/discharging system is used for the experiment. Its configuration is shown in Fig. 11. Originally, the primary side of the DAB converter is connected to the battery and the secondary side is connected to the single phase grid via a separate DC-AC converter. However, in the experiment, a variable DC voltage source is connected to the primary side, and a
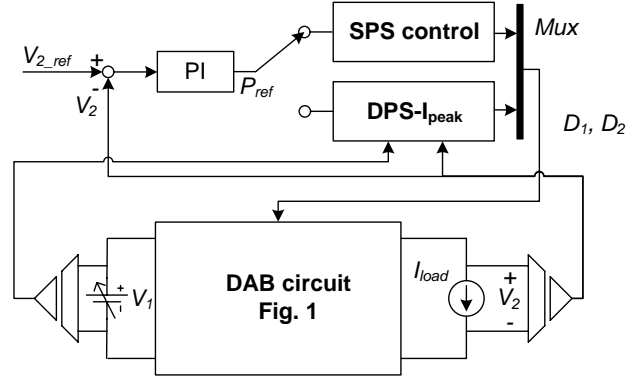

Fig. 11. Configuration of the experimental set

variable current source is connected to the secondary side. The DC-link voltage of primary side is set by the voltage source and the secondary side DC-link voltage is regulated with a voltage controller. The controller produces the output power reference, which is converted into the phase-shift pair according to the control strategy.

The DAB circuit is made of H-bridge modules (F4-75R06W1E3, IGBT module of Infineon) and high frequency transformer. Parameters of the system are the same as the case of the simulation, as shown in Table I. A DSP and a FPGA are used to implement the voltage controller and a gating signal generator.

The experiment is performed under the same condition of the simulation (d=1.78, V_1=200V, V_2=400V). Overall system efficiency is measured while from 10% to the 100% of the rated power is applied using the SPS control strategy and DPS-I$_{peak}$. Results are illustrated in Fig. 12. As expected, the DPS control achieves increased efficiency than the SPS control in low and medium power range.

Fig. 12. Efficiency comparison of SPS and DPS-I$_{peak}$

(a) SPS

(b) DPS-I$_{peak}$

Fig. 13. Voltage and current waveform applied to the transformer

Fig. 13 shows the voltage and current waveform applied to the transformer with SPS control and DPS-I$_{peak}$ when 60% of rated power is transferred. It is clearly confirmed that peak current with DPS-I$_{peak}$ is lower than the case of SPS control. The improvement of ZVS condition is also verified. In Fig 13 (a), only two legs of secondary side H-bridge experience ZVS at t_2 and t_4. While, three legs experience ZVS in Fig 13 (b), where ZVS is occurred at t_2, t_3, and t_4.

VI. CONCLUSIONS

The DPS control strategy for the DAB converter has one more degree of freedom than the conventional SPS control strategy. It controls the duty ratios of the output voltages of the H-bridges by adjusting the phase-shift between half-bridges in the identical side as well as phase-shift between the primary and the secondary side. In order to select the phase-shift pair for a certain output power using DPS control, a proper criterion is required. This paper suggests the reactive power, the rms and peak current, and the ZVS condition as performance indices and analyzes their distribution according to the phase-shift pair and the voltage ratio between the primary and the secondary side. Also, optimum trajectories for each performance index are obtained by analytic calculation or look-up tables. Each trajectory has different shape, thus one of them should be chosen. Simulation result presents that the optimum trajectory for the minimum peak current can be a general solution considering the overall performance and easiness of the implementation. Experiments are performed to verify the proposed control strategy and compare with the conventional SPS control strategy. The experimental results show satisfactory result in terms of overall efficiency and ZVS range.

REFERENCES

[1] M. Jain, M. Daniele, and P.K. Jain, "A bidirectional dc-dc converter topology for low power application," *IEEE Trans. Power Electron.*, vol. 15, pp. 595-606, July 2000.

[2] K. Wang, C. Y. Lin, L. Zhu, D. Qu, F. C. Lee, and J. Lai, "Bi-directional dc to dc converters for fuel cell system," in *Conf. Rec.* 1998 *IEEE Workshop Power Electronics in Transportation*, pp. 47-51.

[3] H. Li, F. Z. Peng, and J. S. Lawler, "A Natural ZVS Medium-Power Bidirectional DC-DC Converter With Minimum Number of Devices," *" IEEE Trans. Ind. App.*, vol. 39, no. 2, March/April 2003.

[4] R.W.De Doncker, D M. Divan, and M.H. Kheraluwala, "A Three-Phase Soft-Switched High-Power-Desity dc-dc Converter for High-Power Applications," *IEEE Trans. Ind. Appl.*, vol.27, no. 1, January/February 1991

[5] F. Krismer, S. Round, and J. W. Kolar, "Performance optimizing of a high current dual active bridge with a wide operating voltage range," in *Proc. 37th IEEE PESC*, Jun. 2006, pp. 1-7

[6] N. Schibli, "DC-DC converters for two-quadrant operation with controlled output voltage," in *Proc. 9th EPE*, 1999, pp. 1-9

[7] H. Zhou and A. M. Khambadkone, "Hybrid Modulation for Dual-Active-Bridge Bidirectional Converter With Extended Power Range for Ultracapacitor Application," *IEEE Trans. Ind. Appl.*, vol. 45, no. 4, pp. 1434-1442, Jan./Aug. 2009.

[8] H. Bai and C. Mi, "Eliminate Reactive Power and Increase System Efficiency of Isolated Bidirectional Dual-Active-Bridge DC-DC Converter Using Novel Dual-Phase-Shift Control,*" IEEE Trans. Power Electron.*, vol. 23, no. 6, pp. 2905-2914, Nov. 2008.

[9] M.H. Kheraluwala, R.W. Gasconigne, D. M. Divan and E. D. Baumann, "Performance characterization of a high-power dual active bridge dc-dc converter," IEEE Trans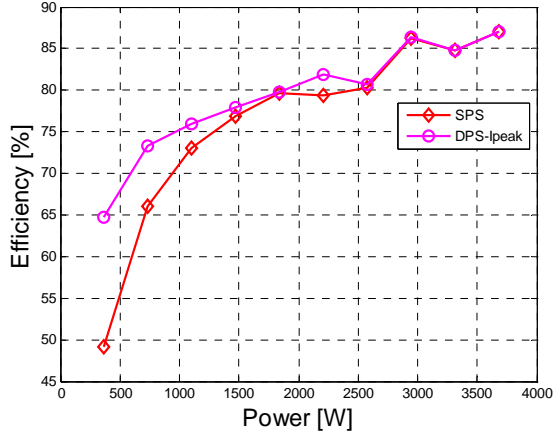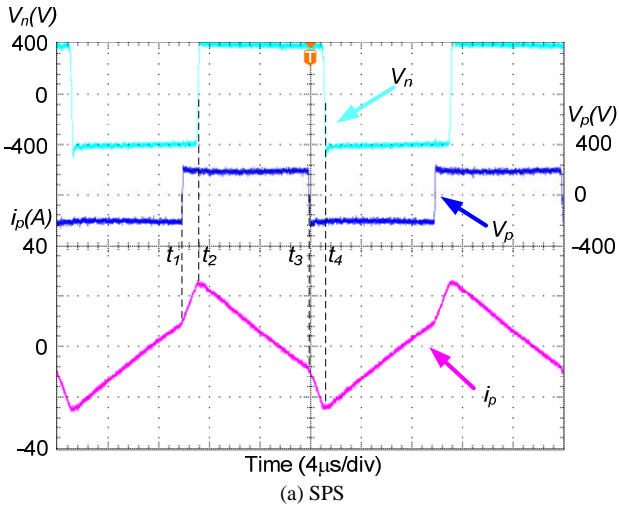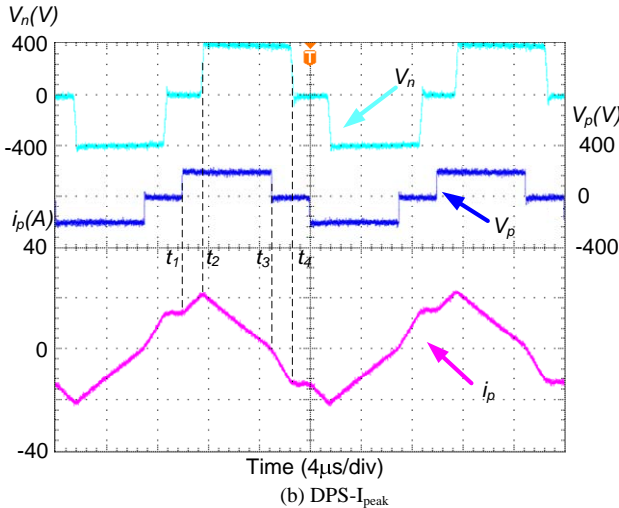. Ind. Appl., 1992, IA-28, pp. 1294–1301